EXCITATIONS OF SUPERFLUID ^{4}He IN CONFINEMENT[a]

B. FÅK
ISIS Facility, Rutherford Appleton Laboratory,
Chilton, Didcot, OX11 0QX, England
and *Commissariat à l'Energie Atomique, DRFMC/SPSMS/MDN,*
38054 Grenoble Cedex 9, France
E-mail:B.Fak@rl.ac.uk

H. R. GLYDE
Department of Physics and Astronomy, University of Delaware,
Newark, Delaware 19716
E-mail: glyde@udel.edu

Neutron inelastic scattering studies of the elementary excitations in confined superfluid ^{4}He are reviewed. Both recent work on helium in porous silica glass (aerogel, Vycor, etc.) and earlier work on helium films on graphite surfaces are discussed. The global picture emerging from these studies is that the three-dimensional excitations are essentially the same as in bulk helium. The characteristic feature of confined helium is the existence of additional layer modes that propagate in the first few liquid layers near the solid-liquid interface. The dispersion and gap energy of these layers modes depend on the substrate. The layer modes are believed to be at the origin of the differences in macroscopic properties compared to bulk helium. Experiments suggest the existence of a localized condensate in Vycor.

1 Introduction

The impact of confinement and disorder on the superfluid and thermodynamic properties of liquid ^{4}He has been a topic of great interest since the 1960s.[1–4] The superfluid transition temperature T_c of liquid ^{4}He in porous media and confined to surfaces is depressed below the transition temperature in bulk liquid ^{4}He, $T_\lambda = 2.172$ K. In fully filled aerogel, Vycor, and Geltech silica, for example, $T_c = 2.167$ K,[5] 1.95–2.01 K,[5,6] and 0.725 K,[7] respectively. Also, the temperature dependence of the superfluid density $\rho_S(T)$ below T_c can be significantly modified. At low enough coverage, ^{4}He in Vycor behaves like an ideal gas.[8]

The characteristic phonon-roton excitations in bulk superfluid ^{4}He have been actively studied by neutron scattering since 1957. Landau initially proposed the existence of excitations in superfluid ^{4}He having energies of the phonon-roton form (see Fig. 1) as a basis for his remarkable theory of superfluidity.[9] In contrast, London proposed that Bose-Einstein condensation (BEC) was the origin of superfluidity.[10] The existence of a condensate is also sufficient to produce a dispersion curve of the phonon-roton form in a Bose fluid.[11,12] In bulk liquid ^{4}He, superfluidity, BEC, and well defined phonon-roton excitations all disappear at the same temperature, T_λ.

The nature of the excitations in porous media is similarly of great interest. Confinement and disorder offer a new arena in which T_c and $\rho_S(T)$ are modified to

[a]Chapter 10 in "Microscopic Approaches to Quantum Liquids in Confined Geometries" ed, E. Krotscheck and J. Navarro, vol. 4 of "Advances in Quantum Many-Body Theory" (World Scientific, Singapore, 2001).)

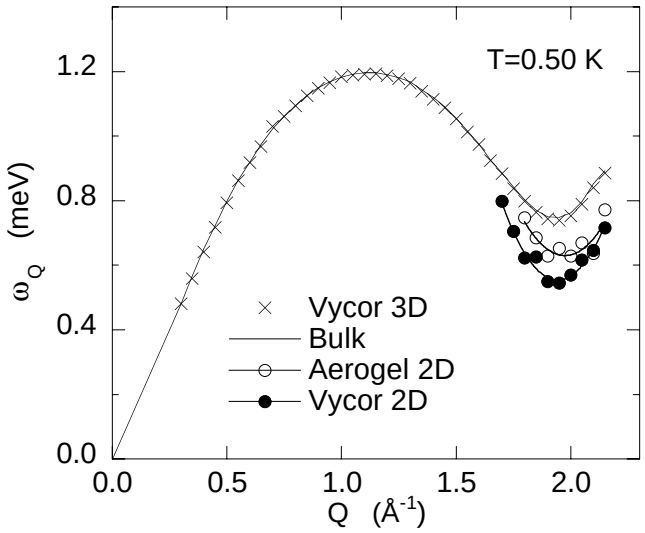

Figure 1: Dispersion curve of the elementary excitations in superfluid ^{4}He in confinement. The three-dimensional (3D) phonon-roton curve is the same in bulk liquid ^{4}He (line) as for helium in Vycor (crosses) and in aerogel (not shown). The open and solid circles show the dispersion for the two-dimensional (2D) layer modes in aerogel and Vycor, respectively, which propagate in the liquid helium layers adjacent to the media walls.

explore the relationship between the condensate, the excitations, and superfluidity. In two dimensions (2D), the loss of superfluidity is attributed to the unbinding of vortex pairs.[13] Below T_c, $\rho_S(T)$ is related to the density of vortices with no clear connection to BEC or to the density of (phonon-roton) excitations. As 2D films thicken, there will be a crossover from 2D to 3D behavior. The study of phonon-roton excitations in films on surfaces and in porous media as a function of film thickness is therefore most interesting.

Equally, liquid ^{4}He in porous media is a model example of "bosons in disorder", which can be related to other dirty Bose systems.[14] Predictions of the impact of disorder on the excitations can be tested.[15] Similarly, calculations of the structure and the excitations of liquid ^{4}He on surfaces have been made,[16,17] as well as predictions of the roton gap energy in two-dimensional ^{4}He.[18,19] These can be tested directly against neutron scattering data.

It is only relatively recently that the elementary excitations of superfluid ^{4}He in confinement and disorder have been successfully studied by neutron scattering. Different types of media have been investigated. Examples are randomly or partly oriented graphite surfaces and disordered porous media with a large variety of porosity, pore sizes, and pore-size distributions. The porous media include different types of aerogel, xerogel, Vycor, and Geltech silica. The excitations of helium in these media show very strong similarities, even between media with flat surfaces such as graphite and media with irregular surfaces such as aerogel. This observation suggests that a global picture of the excitations in confinement can be presented. Unfortunately, reading the original literature without some guidance can be mis-

leading, since the neutron scattering measurements have been difficult and full of pit falls. For these reasons, we believe it is timely to review the experimental results of the excitations in confined helium.

The aim of this review is to present a unified picture of the most significant neutron scattering results of the excitations of superfluid ^{4}He in confinement and disorder. We will not discuss the dynamic properties of ^{3}He in confinement,[20] nor measurements at high wave vectors Q, which probe single-particle properties (atomic momentum distributions) rather than collective dynamics. The review is organized as follows. The global picture emerging from neutron scattering studies of superfluid ^{4}He confined in different media is presented in Sec. 2. Section 3 identifies the pit falls and difficulties in the analysis of the data and discusses general experimental aspects. Many of the original results presented in the literature are in fact artefacts of the data analysis. The understanding of these effects has been a crucial ingredient in arriving at the global picture presented in this review. The following sections 4–6 treat the results from the different media: graphite, aerogel, and Vycor, respectively. Finally, Sec. 7 discusses some interpretations and open questions and identifies some areas where further experimental and theoretical work is needed.

2 Global picture

In this section, we present a global picture of the excitations of superfluid ^{4}He in confinement. References to the literature can be found in the more detailed account of the experimental results in Secs. 4–6. Superfluid ^{4}He in all media studied to date supports well defined three-dimensional (3D) phonon-roton-like excitations. The energies and widths (inverse lifetimes) of these excitations, when carefully analyzed, are the *same* as in bulk helium within current available precision. In particular, the temperature dependence of the excitation energies and widths and the wave-vector dependence of the intensity in the modes are the same as in bulk helium. No well-defined 3D excitations are observed until the equivalent of 1.5 liquid layers of ^{4}He coat the surfaces (substrate plus solid layers). The only significant differences from the bulk occur when the coverage (filling) is reduced: it seems that the maxon energy in liquid ^{4}He on graphite decreases and that the roton energy in aerogel increases. Both these observations suggest the presence of low-density helium layers for thin films.

A particularly interesting observation concerning the 3D excitations is that the temperature dependence of the dynamic structure factor $S(Q,\omega)$ of ^{4}He in Vycor is similar to that in bulk ^{4}He while the superfluid transition temperature T_c is lower. This means that well-defined excitations persist above T_c, suggesting the existence of a localized condensate for temperatures $T_c < T < T_\lambda$.

All systems studied show the existence of layer modes, or indirect signs thereof. Layer modes are two-dimensional (2D) excitations propagating in the first liquid layers close to the media walls, i.e. close to the solid-liquid interface. In all media, the layer modes give rise to a relatively broad peak in $S(Q,\omega)$. There is either one broad or several sharp modes. The layer modes have a roton-like dispersion in dense aerogels and in Vycor, where they are observed only near the roton wave vector ($Q_R = 1.925$ Å^{-1}). On graphite, it seems that both dispersive and dispersionless

(flat) layer modes are observed. Typical 2D roton (gap) energies are 0.55 meV on graphite and in Vycor, and 0.63 meV or higher in aerogel. The intensity of the layer modes starts to grow when there are approximately 1.5 liquid layers present, and saturates at a filling of about 4–5 liquid layers.

Another type of 2D excitation is also seen on flat surfaces such as graphite. Here, a strongly dispersive excitation originating from the free surface (the liquid-gas interface) is observed. It corresponds to a ripplon, which is a quantized capillary wave.

A general observation is that the first 1–1.5 liquid layers do not support any well-defined excitations, neither 2D nor 3D, in any of the media studied. These layers appear "inert", despite being liquid. They sit on top of the solid layer(s). On graphite, there are two crystalline layers with different densities, while it is believed that there is only one amorphous layer in aerogel and Vycor, if one can talk of layers in these cases with irregular surfaces.

3 Experimental aspects

The effects of confinement on the 3D phonon-roton excitations are very small or perhaps absent. Special care is thus needed in analyzing these excitations. Additional intensity in the tails of the phonon-roton peak arising from layer modes or from multiple scattering can easily be mistaken for shifts and broadenings of the peak, if not identified and accounted for in the analysis. Such problems have hampered many of the neutron scattering experiments of superfluid ^{4}He in almost all of the confining media studied. These experimental aspects will be briefly discussed in this section.

The presence of hydrogen, probably in form of OH^- groups bound to the surfaces of aerogel and Vycor, results in strong isotropic incoherent elastic scattering and leads also to multiple scattering: the inelastic scattering of a neutron by ^{4}He is followed or preceded by elastic scattering from the hydrogen. This type of multiple scattering destroys the Q information of $S(Q,\omega)$ from the ^{4}He, but does not change the energy transfer. Its signature is therefore a phonon-roton density-of-states like feature (see Fig. 2). Fortunately, this contribution can be accurately identified and subtracted from the data by comparing with the scattering from bulk ^{4}He at selected wave vectors, in particular at low wave vectors. A problem is that the multiple scattering depends on temperature, since the density-of-states of the phonon-roton excitations depends on temperature. Measurements of ^{4}He on graphite suffer from similar problems, with additional complications coming from the Bragg peaks of the substrate, which introduce a stronger Q dependence of the multiple scattering.

The amount of multiple scattering can be reduced by deuterating the samples in the case of aerogel. The most common method is to flush the aerogel with deuterium gas at relatively high temperatures, which partly replaces the hydrogen by deuterium. Even better results are obtained by making the aerogel from deuterated chemicals and ensuring that it is never exposed to air. In standard Vycor, multiple scattering is not a problem, since the absorption from B_2O_3 impurities is high. However, this absorption also severely reduces the scattered intensity from the ^{4}He, and the key to the most successful experiments on Vycor was to use a

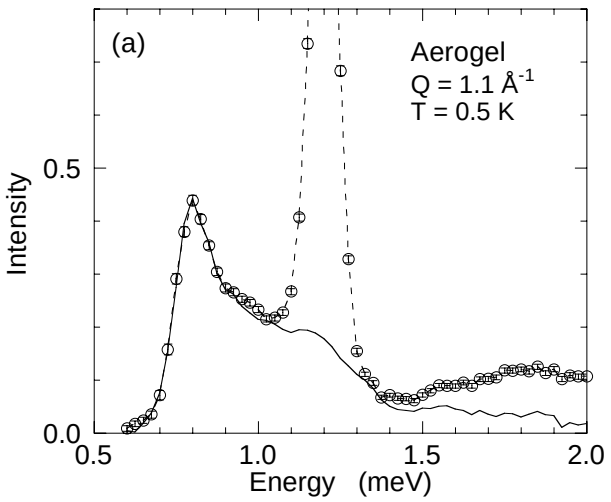

Figure 2: The multiple scattering (solid line) from helium in aerogel (extracted at low wave vectors) resembles the phonon-roton density of states and is essentially Q independent in aerogel and Vycor. The circles and dashed line are the raw data at the maxon wave vector before the multiple scattering is subtracted. As seen, all scattering at energies below the peak is due to multiple scattering. The broad feature at higher energies is the multiphonon contribution.

non-absorbing boron isotope in the fabrication process.

It is also important to avoid having too much bulk liquid around the sample. One method is to use aerogels grown in-situ in the neutron scattering cells, thereby reducing the amount of helium between the aerogel and the cell walls. Another method is underfilling, where the sample is filled only to about 95% of the full capacity, which requires precisely known adsorption isotherms for the actual sample used. This method has the advantage of reducing the amount of helium in cracks in the sample, but increased care is needed to ensure thermal equilibrium.

Since the effects of confinement are small, it is necessary to have accurate measurements of the bulk liquid, made under conditions identical to the measurements of the confined system, and preferentially at the same time. An accurate calibration of the thermometers is also needed. The best method is probably to calibrate the thermometers in-situ, using the vapor pressure of ^{3}He, as was done by some groups. A good thermal contact between the sample and the thermometer(s) is also required, and it appears that certain experiments have given unreliable results due to problems of this type.

When finally extracting the 3D phonon-roton energies and widths from the data, after having corrected for the multiple scattering and including a model for the layer modes, it is essential to use the same fitting procedure for both the confined ^{4}He and the bulk data. Two methods are routinely used, the so-called Wood-Svensson (WS) method and the simple subtraction (SS) method.[21] They have both their shortcomings, but it has been found that the SS method gives the same results independent of the instrumental resolution, while the results of the WS method depend on the resolution. A final remark: it is easier to analyze 3D phonon-roton

excitations in very high-resolution measurements, at least at low temperatures, as the height of the main peak is then so high that the multiple scattering and the layer modes will have a much smaller effect.

4 Films on graphite

Historically, the first neutron scattering studies of the excitations in confined helium considered films on graphite substrates. Measurements began with the pioneering studies of Lambert *et al.*[22] at the Institut Laue-Langevin (ILL) and the early work of Carneiro *et al.*[23] and Thomlinson *et al.*[24] at Brookhaven National Laboratory. Since the 1980s, there has been a major ongoing program at the ILL.[25–32]

Different graphite substrates with large surface to volume ratio have been used over the years. They are all characterized by having flat graphite surfaces with the hexagonal c axis perpendicular to the surface. These surfaces are more or less aligned depending on the material. The most common substrates are graphitized carbon powder (Graphon) and exfoliated and recompressed graphite (Grafoil or Papyex), the latter being more homogeneous and uniform.[20] The results for the ^{4}He excitations are slightly different for different materials, but these differences are not significant compared to the difficulties of analyzing and interpreting the neutron scattering data. In films of at least 4 layers of ^{4}He on exfoliated graphite, the first two layers are solid, forming 2D triangular lattices with densities of 0.115 atoms/Å^2 and 0.095 atoms/Å^2, respectively.[27,30] Subsequent layers are liquid with densities of approximately 0.078 atoms/Å^2,[30] which is similar to the density of bulk liquid ^{4}He at saturated vapor pressure (SVP). It is possible that the third layer has a slightly higher density.[24] Graphite preplated with two solid layers of Ne or H_2 has also been investigated.[26,27,29] The third layer is then liquid or possibly partly solid ^{4}He. There appears to be no significant difference in the excitation spectrum between preplated graphite and ^{4}He-only systems.

The first measurements focused on the excitations at wave vectors in the roton region.[22,23] No well-defined peaks in $S(Q,\omega)$ were seen until four layers (two liquid layers) were deposited. For two or more liquid layers, $S(Q,\omega)$ showed a well-defined peak interpreted as arising from the excitation of a bulk-like 3D roton. Additional intensity below the 3D roton energy was also observed,[22] which was interpreted as the 2D roton predicted by Padmore.[18] Although the poor statistics prevented further interpretation, the measurements by Lambert *et al.* showed all the basic features.

Measurements with much improved statistics were performed by Thomlinson *et al.*[24] They showed that the additional intensity originated from excitations in the first 2–5 liquid layers and was therefore indeed due to a 2D "layer" mode, propagating in the first few liquid layers. The integrated intensity in the layer mode increased with increasing coverage and saturated after 3–4 liquid layers were deposited (see Fig. 3). They also showed that the main peak in $S(Q,\omega)$ was a bulk mode, the 3D roton. At SVP the energy of the 2D roton was 0.54 meV compared to the 3D roton energy of 0.742 meV. No well-defined excitations were observed in films of 1.5 liquid layers or less.

Lauter, Godfrin, and collaborators have reported extensive measurements of

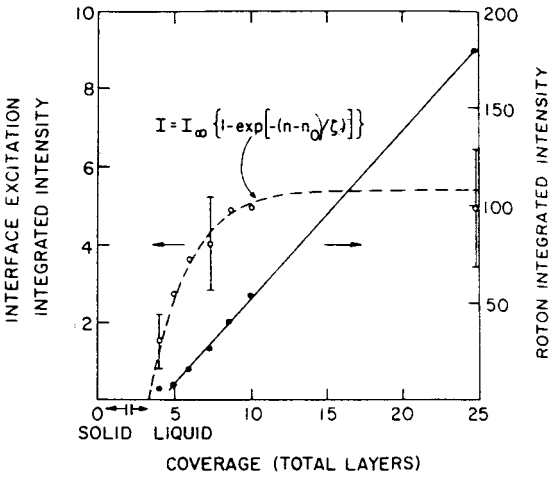

Figure 3: Integrated intensity of the 3D bulk-like roton (solid circles and line) and the 2D layer mode (open circles and dashed line) as a function of helium film thickness on graphite. From Thomlinson *et al.*[24]

excitations in liquid ^{4}He films on graphite.[25–32] Their data at the roton wave vector for thin films (2–8 liquid layers) confirm previous results: a 3D bulk-like roton plus additional intensity attributed to layer modes. Most importantly, their measurements were extended to the phonon and maxon regions, covering wave vectors between 0.25 and 2.0 Å^{-1}. In addition to the 3D rotons and the 2D layer modes, a new mode was discovered, the ripplon.[29,30,31] The ripplon, which can be viewed as a quantized capillary wave, propagates along the surface of the free liquid. The atomic displacements in the mode are perpendicular to the liquid-vapor interface. At low wave vectors, the ripplon dispersion relation is $\omega^2 = (\alpha/\rho)Q^3$, where α is the surface tension and ρ is the liquid density.[33] At wave vectors observable by neutrons the dispersion is approximately linear in Q, up to $Q \approx 1$ Å^{-1} where the ripplon energy flattens and reaches a maximum value of approximately 0.7 meV at $Q = 1.5$ Å^{-1} (see Fig. 4). The ripplon is not clearly separated from the layer modes beyond $Q = 1.5$ Å^{-1}. Lauter *et al.* demonstrated elegantly that the layer modes originate from the solid-liquid interface[26] and that the ripplons originate from the liquid-gas interface (free surface).[31] They found that the layer modes persisted while the ripplons disappeared when the free surface was suppressed by filling the sample completely with liquid ^{4}He. Thus, liquid ^{4}He films support three excitations: a 2D ripplon on the liquid surface, a 3D phonon-roton mode within the liquid film, and 2D layer modes propagating in the liquid layers adjacent to the solid-liquid interface near the substrate.

In what follows, we summarize the main experimental findings concerning the 3D bulk-like excitations and the 2D layer modes of ^{4}He films on graphite, based on the available literature.[22–32] The energy and width (inverse lifetime) of the 3D excitations are very similar to those in bulk helium. In some work, small changes in the energy or the width have been reported, but in most cases these certainly arise

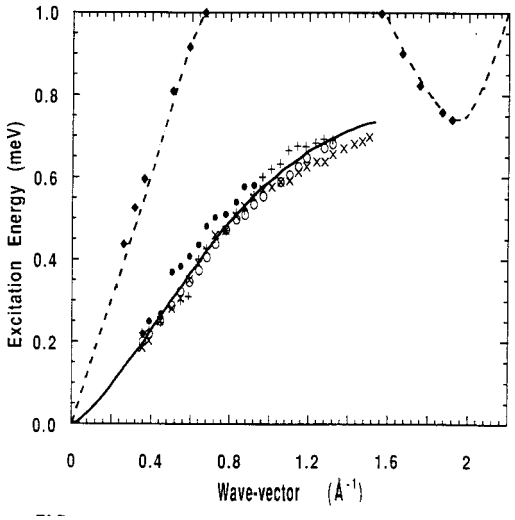

Figure 4: The ripplon dispersion (symbols and solid line) for different film thicknesses of ^{4}He on graphite. The dashed line with symbols is the 3D bulk roton in the cell completely filled with helium. From Lauter *et al.*[31]

from the additional intensity in the tails of the main peak. These tails originate from layer modes or from multiple scattering. In work where corrections for the multiple scattering have been made and the layer modes have been incorporated in

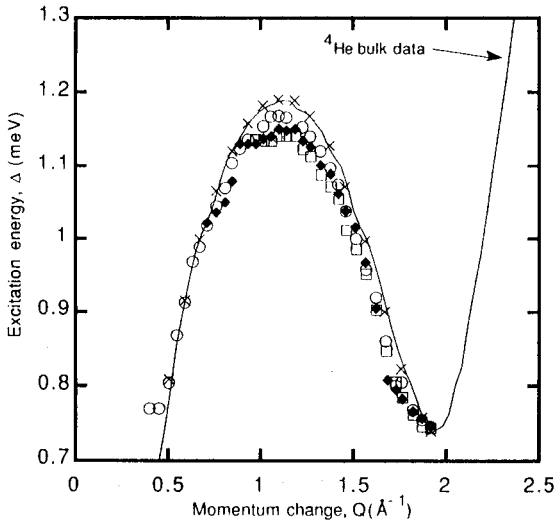

Figure 5: Dispersion relation in the maxon region for different film thicknesses of ^{4}He on graphite. The maxon softens with reduced film thickness. The crosses are data from the cell completely filled with ^{4}He and the line is bulk data. From Lauter *et al.*[30]

the fitting, the energy and width of the 3D excitations are identical to bulk helium. The only exception is possibly the softening of the maxon observed as the coverage is reduced, as shown in Fig. 5.[29,30] This softening suggests the existence of low-density layers in thin films of helium on graphite, while the opposite might be expected. The integrated intensity of the 3D excitations scales linearly with the amount of condensed helium, and extrapolates to zero at approximately 1.5 liquid layers (see Fig. 3).[24] There are indications that the phonons disappear somewhat quicker than maxons and rotons as the coverage is reduced.[29,30] This could be because long wavelength phonons need longer defect-free regions to propagate than rotons, which have a wavelength of the order of atomic distances.

Two-dimensional layer modes propagate in the first few liquid layers close to the substrate. Their integrated intensity scales initially with the amount of condensed liquid, saturates at about 3–4 liquid layers, and extrapolates to zero at approximately 1–1.5 liquid layers (see Fig. 3).[24] The intensity of the layer modes is very weak, making a quantitative analysis difficult. Also, above the roton energy, multiple scattering contributions makes any extraction of layer modes highly uncertain. Several layer modes seem to be observed. Lauter *et al.* reported dispersionless modes that would correspond to excitations perpendicular to the substrate.[26–30] Such flat modes might explain the small Kapitza resistance observed in ^{4}He. The work of Clements *et al.* shows several modes below the roton energy.[32,34] A slightly dispersive branch is seen between the ripplon and the 3D phonon mode for wave vectors below 0.8 Å^{-1}. Near the roton wave vector, one broad or two sharp, slightly dispersive modes are observed, similar to those in aerogel and Vycor. The gap energies of these modes are 0.5 and 0.6 meV, respectively, if we follow the assumption of Clements *et al.* that there are two sharp modes. Thomlinson *et al.*[24] resolved only one layer mode at the roton wave vector with an energy of 0.54 meV.

Calculations suggest that helium layers on surfaces support a two-dimensional layer mode with a phonon-roton-like dispersion.[17,32] Krotscheck *et al.* also report dispersionless modes that are essentially standing modes propagating between the film surface and the solid layer.[17] The energy of these modes would presumably depend on the film thickness. However, it is difficult to determine with precision the energies of the dispersionless modes reported by Lauter *et al.*[29,30] Thus, while the additional intensity observed in the roton region is entirely consistent with a layer mode, the situation is less clear concerning the energy. It would be interesting with experimental and theoretical studies of the temperature dependence of the excitations of helium on graphite.

5 Aerogel

Aerogels are porous solids formed by a sol-gel process. They have a highly tenuous structure of irregularly connected silica (SiO_2) globules and strands with a large distribution of pore sizes, from a few Å to a few hundred Å,[35] and a mean free path of typically 1000 Å. Porosities range from 87 to 99.5%. Small-angle x-ray and neutron diffraction measurements show fractal-like correlations on length scales up to 650 Å. Macroscopic measurements show that the superfluid transition temperature is decreased below T_λ by only 5 mK while the critical exponent for the superfluid flow

density increases from 0.67 in bulk helium to 0.75 for helium in aerogel.[5] There has been no detailed published work on the structure of the helium layers in aerogel, but it appears as if only the first layer forms a solid, an amorphous solid, all other layers being liquid.[36]

Neutron scattering studies of the excitations of ^{4}He in aerogel and other porous media began much more recently (1994) than studies of films on graphite. The first measurements were made by Coddens and collaborators at the Laboratoire Léon Brillouin (LLB),[37,38] soon followed by measurements at the ISIS spallation source (and at the ILL) by Sokol, Stirling, and collaborators.[39–45] Experiments were also performed by a group at the ILL.[46–53] Already the first experiments showed that multiple scattering (see Sec. 3) was a major problem for the interpretation of the data. Much improved results are obtained if it is identified as in Fig. 2 and subtracted, or if deuterated samples are used to substantially reduce it.[46,51,52]

Coddens and collaborators studied both base-catalyzed and neutral-reaction aerogels of 96–96.5% porosity, partially or fully filled with superfluid helium at temperatures of 1.6–1.8 K.[37,38] They elegantly demonstrated that the broad Q-independent scattering centered at the roton energy was due to multiple scattering, as it disappeared when the incident neutron wave vector was made too low to excite the roton. The multiple scattering was relatively strong despite the deuterium-gas treatment of the samples. Due to the limited counting statistics and the coarse energy resolution of $\Delta E = 160\,\mu$eV, no difference was found between the excitation spectrum of helium in aerogel and bulk ^{4}He.

Sokol, Stirling, and collaborators made most of their measurements[39–44] on the backscattering spectrometer IRIS at ISIS, which has a high energy resolution of 15–20 μeV and a rather coarse Q resolution. They used non-deuterated aerogels with 90 and 95% porosity, for which the multiple scattering was an order of magnitude higher than the best samples available.[46] The measurements were performed at temperatures between 1.3 and 2.3 K on slightly underfilled samples, to ensure that no bulk liquid was present. They found initially an increased broadening with temperature of the 3D phonon-roton excitations compared to bulk ^{4}He.[39] This effect is probably due to thermalization problems and/or that the bulk ^{4}He reference run was not made at the same time, and hence under slightly different conditions. Their finding that the temperature dependence of the roton energy was not the same for helium in aerogel and bulk ^{4}He,[40,42] has not been confirmed.[51] It appears as if thermalization problems of the cryostat might be at the origin.[54] No layer modes were observed, which is not surprising in view of the limited signal-to-noise ratio on IRIS at that time. The roton in 95% porous aerogel was measured for temperatures between 0.077 and 1.2 K with very high energy resolution, $\Delta E \sim 1$ μeV, using the IN10 spectrometer at the ILL.[45] Measurements in a related system, 72% porous xerogel, have also been made on IN6 at the ILL as a function of coverage at $T = 1.25$ K.[55]

The group at the ILL made most of their measurements on the IN6 time-of-flight spectrometer ($\Delta E \approx 110\,\mu$eV) and on the IN12 triple-axis spectrometer ($\Delta E = 46$ or 110 μeV) at temperatures between 0.5 and 2.25 K.[46–52] They used aerogel samples of 87 and 95% porosity that were either fully deuterated or deuterium-gas treated to reduce multiple scattering. The aerogels were grown directly in the sample cells

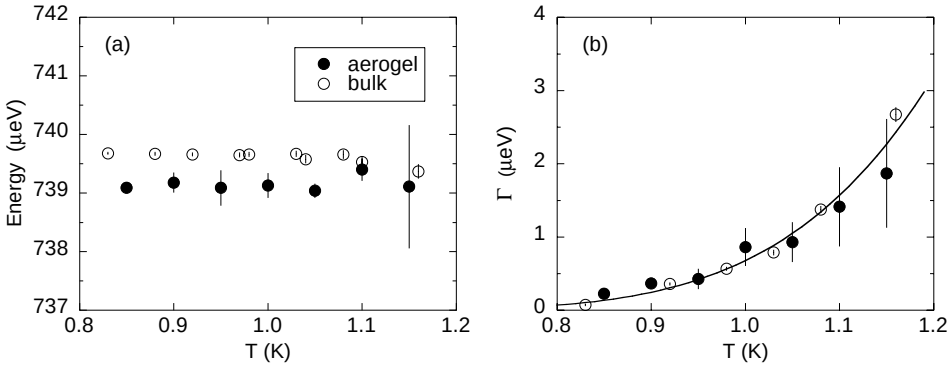

Figure 6: Temperature dependence of the 3D roton energy (a) and line width [HWHM] (b) for superfluid helium in aerogel (solid circles) and in bulk ^{4}He (open circles) from the high-resolution measurements of Anderson *et al.*[45]

used for the neutron scattering measurements to reduce the amount of bulk liquid, and the thermometers were calibrated against the ^{3}He vapor pressure. Bulk ^{4}He reference measurements were made simultaneously. Small shifts and broadenings of the phonon-roton excitations in aerogel were initially found with respect to bulk helium.[46] However, these effects arised from additional scattering by layer modes, which were not identified at that time.[51] Measurements beyond the roton wave vector ($Q \gtrsim 2.4$ Å^{-1}) were made on IN12 [46] and on IRIS,[53] using the same fully deuterated sample.

We will now discuss the main results of the above mentioned neutron scattering experiments on helium in aerogel. These measurements show that superfluid ^{4}He in aerogel (fully filled) supports well-defined 3D phonon-roton excitations at low temperatures ($T \lesssim 1.4$ K). These excitations are identical to those in bulk helium, within the precision of present neutron scattering techniques.[45,51] The small modifications of the excitation energy and width reported in early work most likely arise because additional intensity in the tails of the main phonon-roton peak was not recognized and subtracted. If this additional intensity is accounted for, the 3D excitations are the same as in bulk helium. The additional scattering is due to layer modes or multiple scattering. Measurements with sufficiently high energy resolution allows the separation of the main peak from the tails. This was very convincingly shown in the high-resolution measurements of Anderson *et al.* (see Fig. 6).[45] They found that the intrinsic width of the roton was below 0.1 μeV at low temperatures ($T = 0.08$ K).

The temperature dependence of the 3D phonon-roton excitations of ^{4}He in aerogel is also the same as in bulk helium. This was shown for the intrinsic width by Anderson *et al.*[45] for temperatures up to 1.2 K (see Fig. 6) and for temperatures up to 2 K by Plantevin *et al.*[52] The temperature dependence of the 3D roton energy in aerogel is also the same as in bulk, as clearly shown in Fig. 7.[49–52]

The filling dependence of the 3D excitations has also been studied in denser aerogels of 87% porosity.[51] The integrated intensity of the 3D phonon-roton excitation scales with the filling fraction (see Fig. 8), and extrapolates to zero at a total

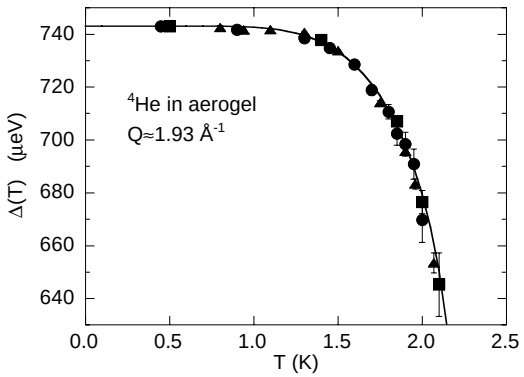

Figure 7: Temperature dependence of the 3D roton energy $\Delta(T)$ in different aerogel samples (symbols) compared to bulk ^{4}He (line). From Fåk *et al.*[51]

of three layers (1–2 liquid layers). The roton energy appears to be higher than the bulk value at low coverages (see Fig. 8), suggesting the existence of low-density layers.

In addition to the 3D phonon-roton excitations, clear evidence for layer modes is seen in denser aerogel, but only near the roton wave vector (see Fig. 9).[51] This is in contrast to helium films on graphite, where layer modes are observed over a

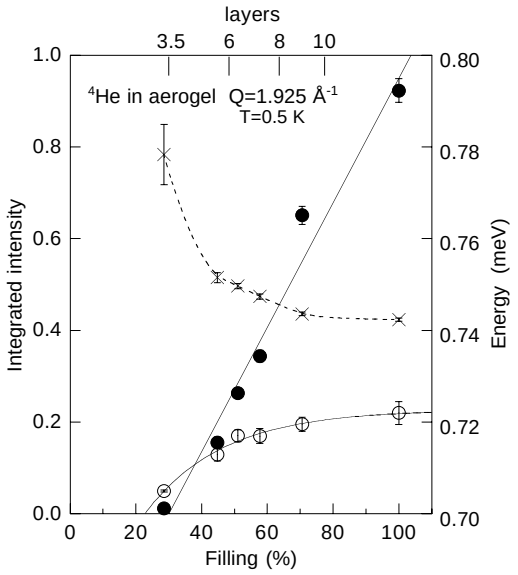

Figure 8: Integrated intensity of the 3D bulk-like roton (closed circles) and the 2D layer mode (open circles) in superfluid ^{4}He in 87% porous aerogel at low temperatures as a function of filling. The solid lines show a linear fit to the 3D mode and a fit of $I(n) = I_\infty\{1 - \exp[-(n - n_0)/\zeta]\}$ to the 2D mode. The crosses show the energy of the 3D bulk-like roton. The dashed line is a guide to the eye. From Fåk *et al.*[51]

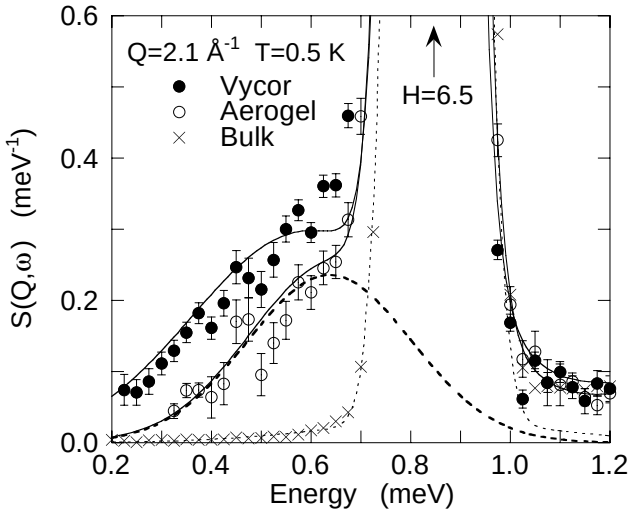

Figure 9: Dynamic structure factor near the roton wave vector for helium in aerogel (open circles) and Vycor (solid circles) compared to bulk ^{4}He (crosses). The 2D layer modes are clearly seen in the low-energy tail ($\sim$ 0.5 meV) of the main 3D phonon-roton peak.

large range of Q values. As for graphite, the additional scattering can be attributed to one broad or several sharp layer modes. The layer modes appear in $S(Q,\omega)$ as additional intensity immediately below the 3D roton peak. The integrated intensity of the layer modes increases with the filling fraction (see Fig. 8). It extrapolates to zero at 3 total layers (1–2 liquid layers), i.e. the same as for the 3D excitations, and saturates at a total of 6 layers. The layer modes have a roton-like dispersion (see Fig. 1) with an energy gap of 0.63–0.72 meV, which is higher than for graphite or Vycor. Different experiments give different values for the gap energy of the layer mode,[51] and it is not clear at present whether different aerogels have different gap energies or if there are several layer modes with different energies.

There are few theoretical calculations that deal with the excitations of superfluid ^{4}He in aerogel. It is not clear how calculations of excitations on flat surfaces carry over to aerogel, which is characterized by irregular surfaces. Aerogel is probably also a rather inhomogenous media, due to the wide distribution of open volume sizes. For partly filled samples, small open regions are likely to fill up and have more layers than larger cavities, due to capillary condensation. It is not clear whether there are one or several layer modes, and theoretical calculations would assist data interpretation.

6 Vycor

Porous Vycor glass is made by leaching out the B_2O_3-rich phase of a phase-separated borosilicate glass. The result is a sponge-like silica-rich material, consisting of an open network of approximately 70 Å diameter channels and with a porosity of about 30%. Due to the fabrication method, Vycor contains approximately 3.5%

B_2O_3. The superfluid transition temperature is suppressed from $T_\lambda = 2.172$ K in the bulk to T_c in the range 1.95 to 2.03 K in Vycor,[5,6] while the critical exponent for the superfluid density is the same as in bulk ^{4}He.[5] It is believed that the first ^{4}He layer on Vycor forms an amorphous solid while subsequent layers are liquid.

The strong neutron absorption of the ^{10}B isotope in the remaining B_2O_3 impurities in Vycor makes neutron scattering experiments very difficult. The first inelastic neutron scattering measurements by Lauter and Godfrin at the ILL and by Coddens and collaborators at the LLB are unpublished. The first successful experiment used fully filled standard Vycor on IN6.[56] This was soon followed by more accurate work (also on IN6) using isotopic Vycor, where the ^{10}B isotope was replaced by non-absorbing ^{11}B.[52,57] The negligible absorption of this particular sample greatly improved the quality of the data and made a quantitative analysis possible, after correction for multiple scattering (which becomes important with reduced absorption).

The results from these measurements are that the 3D phonon-roton excitations are the same in fully filled Vycor as in bulk helium at all temperatures. The indications of an increased width and a modified energy (compared to bulk) as a function of temperature in the absorbing sample are most likely due to poor statistics and unresolved layer modes.[56] No differences in the phonon-roton excitations from the bulk were observed in the non-absorbing sample.[57]

In addition to the 3D excitations, additional intensity is observed near the roton wave vector, interpreted as due to layer modes.[56,57] There are no published results on the filling dependence of the excitations in Vycor, and hence no proof for that this additional intensity comes from two-dimensional excitations. However, the scattering is very similar to the layer modes in aerogel and on graphite, leaving little doubt about its origin (see Fig. 9). The dispersion of the layer modes is roton-like, with a roton gap energy of 0.55 meV (see Fig. 1).[57] This energy is the same as the roton energy of the layer modes of ^{4}He on graphite (0.54 meV), but lower than that in aerogel. Layer modes with an energy of 0.53 meV explain the observed specific heat attributed to helium layers in Vycor.[58]

The biggest surprise was perhaps that the dynamic structure factor $S(Q,\omega)$ for the 3D excitations has a temperature dependence in Vycor similar to that in bulk helium (see Fig. 10), even though the superfluid transition temperature T_c is lower. In particular, well-defined maxons and rotons were observed above the superfluid transition temperature $T_c \approx 1.95$ K in Vycor.[57] Estimates of the dead volume between the Vycor sample and the sample cell and in cracks in the Vycor sample show that the amount of bulk liquid collecting in these volumes cannot account for the observed effect.

If well-defined maxons and rotons is the signature of the existence of a Bose condensate, as proposed in the Glyde-Griffin interpretation,[59,60,61] the observation of such excitations above T_c suggests the existence of a localized condensate above T_c. In other words, between the superfluid transition temperature T_c in Vycor and that of the bulk liquid, T_λ, there is a condensate localized in the larger pores in the sample, and it is only below T_c that different localized condensates connect and allows the superfluid to flow through the sample. We note that T_c is determined by torsional oscillator measurements, which measure the percolating superfluid in

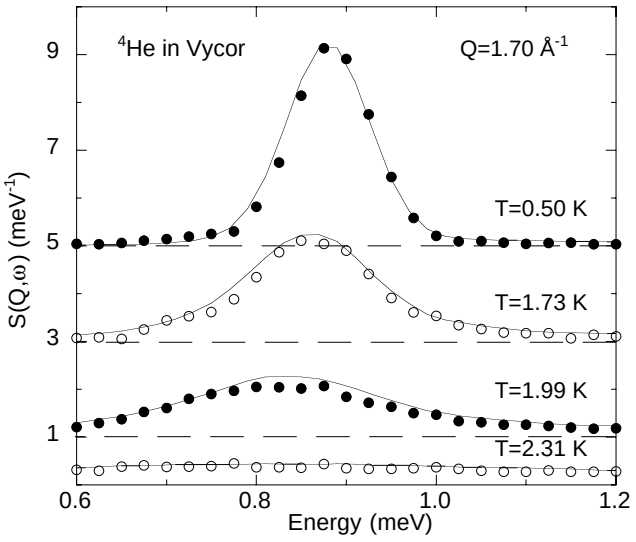

Figure 10: Temperature dependence of the dynamic structure factor of liquid helium in Vycor (symbols) compared to bulk ^{4}He (lines) at a wave vector between the maxon and roton regions. There is clearly a relatively well-defined excitation at $T = 1.99$ K $\gtrsim T_c$ in Vycor. From Glyde *et al.*[57]

the sample. The existence of a localized condensate in helium due to disorder has been predicted theoretically,[62,63,64] and it would be very interesting if its observation could be confirmed. Direct measurements of the condensate fraction in Vycor using high-momentum-transfer neutron scattering are under way.

7 Discussion

The energies and lifetimes of the phonon-roton excitations of superfluid ^{4}He in fully filled aerogel and Vycor are the same as in bulk liquid ^{4}He within current precision (5 μeV). Particularly, the width of the roton excitation is unobservably small at low temperatures ($\Gamma \leq 0.1$ μeV at $T = 0.08$ K) [45] and its temperature dependence is the same as in bulk ^{4}He up to T_λ.[52] Whatever differences have been observed tend to disappear when measured with increased precision and compared with simultaneously measured bulk values.

This result is somewhat surprising since the excitation energies are a sensitive function of the liquid density.[60] It suggests that the liquid density in which the excitations propagate in aerogel and Vycor is predominantly at the bulk SVP density. The excitation energies in superfluid films at low temperatures on graphite are also much the same as in the bulk within observed precision. No 3D phonon-roton excitations propagate until at least 3.5 total (1.5 liquid) layers are deposited on graphite,[24] and until the equivalent of 3.5 total layers in aerogel.[51] On graphite, the fourth layer is believed to be at the bulk density. Thus the layers in which the 3D excitations propagate are probably at bulk density, which is consistent with the equality of the excitation energies in films on graphite and the bulk. Any vari-

ation in density would also introduce a width to the excitations. A finite width for phonons, which propagate with a sound velocity $c \simeq 200$ m/s, is expected in confinement. This has not been observed.

The exceptions to the above findings are: (i) in partially filled aerogel, the roton energy lies above the bulk value;[51] (ii) in films on graphite, the maxon energy may lie below the bulk value for low coverages;[29] and (iii) in Geltech silica, which has 25 Å diameter pores, the excitations appear to differ from bulk values at partial fillings.[65]

There have been several predictions for the change in excitation energies in Bose fluids arising from disorder. In a dilute Bose gas, Zhang predicted that white noise random disorder would reduce the sound velocity of phonons and introduce a width.[66] New excitations at low energy (low $\hbar\omega$), especially at long wavelength, have been predicted when disorder is introduced.[67] Theoretical calculations have suggested that a gap could open up in the phonon dispersion curve in the long wavelength limit in disorder.[63] Plantevin *et al.* searched for a gap and new excitations at low wave vectors ($Q \simeq 0.2$ Å^{-1} corresponding to $\hbar\omega \approx 0.325$ meV) in 95% porous aerogel but found no departure from the bulk.[46] A major problem in this search is that the elastic scattering ($\omega = 0$) even from fully deuterated aerogel samples is still large enough to mask small inelastic contributions at low ω. Boninsegni and Glyde calculated $S(Q,\omega)$ of superfluid ^{4}He containing small (2 Å) hard spheres randomly placed.[68] $S(Q,\omega)$ was both broadened and displaced in energy with new weight at low ω. Apparently, disorder on short length scales is needed to modify $S(Q,\omega)$ significantly.

The new excitations observed in porous media not seen in the bulk are the layer modes. They have been observed in aerogel,[51] xerogel,[55] Vycor,[56,57] and Geltech silica.[65] The layer modes are pictured as 2D "phonons" propagating in the liquid layers adjacent to the media walls. At the roton wave vector at least, the layer modes are the same as those observed in liquid ^{4}He films on graphite.[22,24,32] In porous media, the layer modes have been observed in the wave-vector range $1.7 \leq Q \leq 2.15$ Å^{-1}. In this Q range, they have a "roton-like" dispersion (see Fig. 1). Below $Q = 1.7$ Å^{-1}, the intensity in the mode becomes too small to be observed or the mode overlaps with the phonon-roton peak or the multiple scattering.[52] The mode intensity increases with wave vector up to $Q = 2.15$ Å^{-1}, the maximum value investigated. It would be most interesting to determine whether layer modes exist up to higher wave vectors and what their intensity and dispersion might be. In films on graphite, it seems that both dispersive [32] and dispersionless [29] layer modes are observed. Calculations of films on substrates show propagating dispersive 2D modes.[32]

In Vycor,[57] the 2D roton energy $\Delta_{2D} = 0.55 \pm 0.01$ meV agrees well with the energy of 0.53 meV extracted by Brewer *et al.*[4,58] from the layer contribution to the specific heat. It is also consistent with the gap energy of 0.50 meV obtained by Kiewiet *et al.*[69] from the superfluid density in Vycor for $T \leq 1.4$ K. Further connections between excitation energies observed by neutron scattering and thermodynamic or transport properties would be most interesting. These, however, must be restricted to low temperatures ($T \leq 1.5$ K), where the excitation energies are sharply defined.

In bulk liquid ^{4}He, the integrated intensity in the characteristic phonon-roton excitation for $Q \gtrsim 0.7$ Å^{-1} scales approximately with the superfluid density $\rho_S(T)$. There is no well-defined excitation above T_λ in the normal phase (for $Q \gtrsim 0.7$ Å^{-1}). In Vycor, a well-defined excitation was observed above $T_c \approx 1.95$ K. At $T = 1.99$ K, where $\rho_S(T) = 0$ in Vycor, approximately one half of the intensity is still in the elementary excitation. Glyde and Griffin proposed that the intensity in the elementary excitation should scale as $n_0(T)$.[59] The result in Vycor suggests that there is still some condensate above T_c, perhaps a localized condensate.[64] That is, there could be superfluid Bose-condensed regions on dimensions of the pore size in larger open regions. However, these regions do not extend across the whole media. These locally condensed regions would not be observed in a torsional oscillator measurement.[2,5] Bose-Einstein condensation on short length scales in confinement has been suggested to explain thermal expansion data[70] and discussed theoretically.[64,71] Further theoretical exploration of this interesting concept is needed.

Helium in porous media is subject to both confinement and disorder. The confinement comes from the limited pore size and the quasi-two dimensional character of the media walls/substrate, while the disorder comes from the irregular structures of the pores. A legitimate question is which of these two effects is dominating the changes in the microscopic and macroscopic properties. By comparing the results from ^{4}He in aerogel and Vycor with ^{4}He on graphite, which to a rather high degree presents atomically well ordered planar substrates, a preliminary answer would be that confinement is more important. The reasons are that the 3D excitations are identical in these two types of materials and that the 2D layer modes show many similarities. Theoretical work would be very welcome here, particularly on the length scales of disorder needed to have an impact on the excitations.

Experimentally, work is in progress to study porous media that present long-range order, such as zeolites. Another trend is to go to smaller pore sizes, in order to increase the effects of confinement. The first studies of high-porosity aerogels ($\approx$ 95%) did not permit direct observation of layer modes, although indirect signs were seen such as apparent broadenings and shifts of the 3D excitations. However, in higher density aerogels[51] as well as in xerogel,[55] both with a porosity of 87%, layer modes were observed. Another system which has just started to be investigated is 50% porous Geltech,[65] where the pore size is very small, of the order of 25 Å, and where the superfluid transition temperature is suppressed to 0.725 K.

Acknowledgments

We would like to thank O. Plantevin, J. Bossy, G. Coddens, H. Schober, and R.T. Azuah for very fruitful collaboration on the neutron scattering experiments. These measurements would not have been possible without the efforts of J.R. Beamish, N. Mulders, and D.S. Danielson, who specifically prepared our samples. We have also benefitted from helpful discussions with C.R. Anderson, K.H. Andersen, E. Krotscheck, H. Godfrin, H.J. Lauter, W.G. Stirling, P.E. Sokol, R.M. Dimeo, L. Puech, and E. Wolf. HRG was supported in part by the National Science Foundation through research grant DMR-9972011.

References

1. D.F. Brewer, in *The Physics of Liquid and Solid Helium*, Part II, eds. K.H. Benneman and J.B. Ketterson (Wiley, New York, 1978), p. 573.
2. J.D. Reppy, *J. Low Temp. Phys.* **87**, 205 (1992).
3. M. Chan, N. Mulders, and J. Reppy, *Physics Today*, August 1996, p. 30.
4. D.F. Brewer, *Physica* B **280**, 4 (2000).
5. M.H.W. Chan, K.I. Blum, S.Q. Murphy, G.K.S. Wong, and J.D. Reppy, *Phys. Rev. Lett.* **61**, 1950 (1988).
6. G.M. Zassenhaus and J.D. Reppy, *Phys. Rev. Lett.* **83**, 4800 (1999).
7. S. Miyamoto and Y.Takano, *Czech. J. Phys.* **46**, 137 (1996).
8. J.D. Reppy, B.C. Crooker, B. Hebral, A.D. Corwin, J. He, and G.M. Zassenhaus, *Phys. Rev. Lett.* **84**, 2060 (2000).
9. L.D. Landau, *J. Phys. U.S.S.R.* **11**, 91 (1947).
10. F. London, *Nature* **141**, 643 (1938).
11. N.N. Bogoliubov, *J. Phys. U.S.S.R.* **11**, 23 (1947).
12. J. Gavoret and P. Nozières, *Ann. Phys.* **28**, 349 (1964).
13. J.M. Kosterlitz and D.J. Thouless, *Prog. Low Temp. Phys.* VIIB, 371 (1978).
14. U.C. Täuber and D.R. Nelson, *Phys. Repts.* **289**, 157 (1997).
15. M. Ma, P. Nisamaneephong, and L. Zhang, *J. Low Temp. Phys.* **93**, 957 (1993).
16. B.E. Clements, E. Krotscheck, and C.J. Tymczak, *Phys. Rev.* B **53**, 12 253 (1996).
17. E. Krotscheck, M.D. Miller, and R. Zillich, *Physica* B **280**, 59 (2000).
18. T.C. Padmore, *Phys. Rev. Lett.* **32**, 826 (1974).
19. W. Götze and M. Lücke, *J. Low Temp. Phys.* **25**, 671 (1976).
20. H. Godfrin and H.J. Lauter, *Prog. in Low Temp. Phys.* Vol. XIV, ed. W.P. Halperin, (Elsevier, Amsterdam, 1995), p. 213; H. Godfrin and R.E. Rapp, *Adv. Phys.* **44**, 113 (1995).
21. K.H. Andersen, W.G. Stirling, R. Scherm, A. Stunault, B. Fåk, H. Godfrin, and A.J. Dianoux, *J. Phys. Condens. Matter* **6**, 821 (1994); K.H. Andersen and W.G. Stirling, *ibid.* 5805.
22. B. Lambert, D. Salin, J. Joffrin, and R. Scherm, *J. Phys. (Paris), Lett.* **38**, L377 (1977).
23. K. Carneiro, W.D. Ellenson, L. Passell, J.P. McTague, and H. Taub, *Phys. Rev. Lett.* **37**, 1695 (1976).
24. W. Thomlinson, J.A. Tarvin, and L. Passell, *Phys. Rev. Lett.* **44**, 266 (1980).
25. H.J. Lauter, H. Wiechert, and C. Tiby, *Physica* **107**B, 239 (1981).
26. H.J. Lauter, H. Godfrin, C. Tiby, H. Wiechert, and P.E. Obermayer, *Surface Science* **125**, 265 (1983).
27. H.J. Lauter, H. Godfrin, and H. Wiechert, in *Phonon Physics*, eds. J. Kollar *et al.* (World Scientific, Singapore, 1985), p. 842.
28. H.J. Lauter, V.L.P. Frank, H. Godfrin, and H. Wiechert, in *Elementary Excitations in Quantum Fluids*, eds. K. Ohbayashi and M. Watabe, Springer Series in Solid State Sciences Vol. 79 (Springer-Verlag, Berlin, 1989), p. 99.
29. H.J. Lauter, H. Godfrin, V.L.P. Frank, and P. Leiderer, in *Excitations in Two-*

Dimensional and Three-Dimensional Quantum Fluids, eds. A.F.G. Wyatt and H.J. Lauter (Plenum, New York, 1991), p. 419.
30. H.J. Lauter, H. Godfrin, and P. Leiderer, *J. Low Temp. Phys.* **87**, 425 (1992).
31. H.J. Lauter, H. Godfrin, V.L.P. Frank, and P. Leiderer, *Phys. Rev. Lett.* **68**, 2484 (1992).
32. B.E. Clements, H. Godfrin, E. Krotscheck, H.J. Lauter, P. Leiderer, V. Passiouk, and C.J. Tymczak, *Phys. Rev.* B **53**, 12 242 (1996).
33. D.O. Edwards and W.F. Saam, *Prog. in Low Temp. Phys.* Vol. VII A, ed. D.F. Brewer, (North Holland, Amsterdam, 1978), p. 283.
34. Note that Clements *et al.*[32] present the data at constant scattering angle rather than constant Q as is customary. The wave vectors k given in the paper correspond therefore to elastic scattering, and need to be modified at finite energy transfers.
35. J.V. Porto and J.M. Parpia, *Phys. Rev.* B **59**, 14 583 (1999).
36. H. Godfrin, J. Klier, V. Lauter-Pasyuk, H. Lauter, P. Leiderer, *ILL Experimental Report* 6-01-177 (1998), unpublished.
37. J. de Kinder, G. Coddens, and R. Millet, *Z. Phys.* B, *Condensed Matter* **95**, 511 (1994).
38. G. Coddens, J. de Kinder, and R. Millet, *J. Non-Cryst. Solids* **188**, 41 (1995).
39. M.R. Gibbs, P.E. Sokol, R.T. Azuah, W.G. Stirling, and M.A. Adams, *Physica* B **213-214**, 462 (1995).
40. P.E. Sokol, M.R. Gibbs, W.G. Stirling, R.T. Azuah, and M.A. Adams, *Nature* **379**, 616 (1996).
41. M.R. Gibbs, P.E. Sokol, W.G. Stirling, R.T. Azuah, and M.A. Adams, *J. Low Temp. Phys.* **107**, 33 (1997).
42. R.M. Dimeo, P.E. Sokol, D.W. Brown, C.R. Anderson, W.G. Stirling, M.A. Adams, S.H. Lee, C. Rutiser, and S. Komarneni, *Phys. Rev. Lett.* **79**, 5274 (1997).
43. P.E. Sokol. R.M. Dimeo, D.W. Brown, C.R. Anderson, W.G. Stirling, M.A. Adams, S.H. Lee, C. Rutiser, and S. Komarneni, *Physica* B **241-243**, 929 (1998).
44. R.M. Dimeo, P.E. Sokol, C.R. Anderson, W.G. Stirling, and M.A. Adams, *J. Low Temp. Phys.* **113**, 369 (1998).
45. C.R. Anderson, K.H. Andersen, J. Bossy, W.G. Stirling, R.M. Dimeo, P.E. Sokol, J.C. Cook, and D.W. Brown, *Phys. Rev.* B **59**, 13 588 (1999).
46. O. Plantevin, B. Fåk, H.R. Glyde, J. Bossy, and J.R. Beamish, *Phys. Rev.* B **57**, 10 775 (1998).
47. H.R. Glyde, B. Fåk, and O. Plantevin, *J. Low Temp. Phys.* **113**, 537 (1998).
48. O. Plantevin, Ph.D. Thesis, Université Joseph Fourier, Grenoble, France (1999).
49. B. Fåk, O. Plantevin, and H.R. Glyde, *Physica* B **276-278**, 806 (2000).
50. B. Fåk, O. Plantevin, and H.R. Glyde, *J. Phys. IV (France) Colloque* **10**, Pr7: 163 (2000).
51. B. Fåk, O. Plantevin, H.R. Glyde, and N. Mulders, *Phys. Rev. Lett.* **85**, 3886 (2000).
52. O. Plantevin, B. Fåk, H.R. Glyde, N. Mulders, J. Bossy, G. Coddens, and H.

Schober, submitted to *Phys. Rev.* B.
53. R.T. Azuah, H.R. Glyde, J.R. Beamish, and M.A. Adams, *J. Low Temp. Phys.* **117**, 113 (1999).
54. P.E. Sokol, private communication.
55. C.R. Anderson, W.G. Stirling, K.H. Andersen, P.E. Sokol, and R.M. Dimeo, *Physica* B **276-278**, 820 (2000).
56. R.M. Dimeo, P.E. Sokol, C.R. Anderson, W.G. Stirling, K.H. Andersen, and M.A. Adams, *Phys. Rev. Lett.* **81**, 5860 (1998).
57. H.R. Glyde, O. Plantevin, B. Fåk, G. Coddens, P.S. Danielson, and H. Schober, *Phys. Rev. Lett.* **84**, 2646 (2000).
58. D.F. Brewer, A.J. Symonds, and A.L. Thomson, *Phys. Rev. Lett.* **15**, 182 (1965).
59. H.R. Glyde and A. Griffin, *Phys. Rev. Lett.* **65**, 1454 (1990).
60. H.R. Glyde, *Excitations in Liquid and Solid Helium* (Oxford University Press, Oxford, 1994); *J. Low Temp. Phys.* **93**, 349 (1993).
61. A. Griffin, *Excitations in a Bose-Condensed Liquid* (Cambridge University Press, Cambridge, 1993).
62. D.J. Thouless, *Phys. Rep., Phys. Lett.* **13C**, 93 (1974).
63. W. Krauth and N. Trivedi, *Europhys. Lett.* **14**, 627 (1991); W. Krauth, N. Trivedi, and D. Ceperley, *Phys. Rev. Lett.* **67**, 2307 (1991); T. Giamarchi and P. Le Doussal, *Phys. Rev. Lett.* **76**, 3408 (1996).
64. K. Huang, in *Bose Einstein Condensation*, eds. A. Griffin, D. Snoke, and S. Stringari (Cambridge University Press, Cambridge, 1995), p. 31.
65. O. Plantevin, B. Fåk, and H.R. Glyde, *J. Phys. IV (France) Colloque* **10**, Pr7: 177 (2000).
66. L. Zhang, *Phys. Rev. B* **47**, 14 364 (1993).
67. M. Makivić, N. Trivedi, and S. Ullah, *Phys. Rev. Lett.* **71**, 2307 (1993).
68. M. Boninsegni and H.R. Glyde, *J. Low Temp. Phys.* **112**, 251 (1998).
69. C.W. Kiewiet, H.E. Hall, and J.D. Reppy, *Phys. Rev. Lett.* **35**, 1286 (1975).
70. P. Thibault, J.J. Préjean, and L. Puech, *Czech. J. Phys.* **46**, 149 (1996).
71. K. Huang and H.-F. Meng, *Phys. Rev. Lett.* **69**, 644 (1992).